JOURNAL OF MATERIALS SCIENCE 32 (1997) 2623–2627

Crystallization kinetics of fluorophosphate glasses

Part I *Effect of composition and heating rate*

A. OZTURK
Metallurgical and Materials Engineering Department, Middle East Technical University, Ankara 06531, Turkey

Crystallization behaviour of glasses from the system AlF_3–MF_2–$Ba(PO_3)_2$ (M = Ca, Mg, Sr, Ba) have been studied using differential thermal analysis as a function of $Ba(PO_3)_2$. The kinetic parameters for crystallization, namely, the activation energy, E, frequency factor, ν, and Avrami exponent, n, were determined. E, ν and n decreased with increasing $Ba(PO_3)_2$. Crystallization commenced at higher temperatures and the crystal growth mechanism changed from bulk to surface with increasing $Ba(PO_3)_2$. X-ray diffraction analysis revealed that $CaAlF_5$, $SrAlF_5$, $CaAlF_7$ and $CaSrAlF_7$ crystallize from these glasses when heated. The infrared transmission spectra indicated that AlF_6, PO_3F and $Ba(Ca,Mg,Sr)P_2O_7$ groups were present in these glasses.

1. Introduction

Materials with good optical characteristics are of great importance for the construction of high efficiency optics. For this reason attempts are being made to find glasses with improved optical properties.

Fluorophosphate glasses are a kind of new optical glasses with superior optical properties such as low refractive index with high Abbe number, large anomalous partial dispersion, low non-linear refractive index and high transmittance in near ultraviolet (UV) and infrared (IR) regions [1–5]. The combination of these properties makes these glasses useful for high energy laser systems (undoped lenses, turning mirrors, filters, Faraday rotators, laser windows). Also they find special applications such as components of IR domes, mid-IR optical fibres and polarizing substrates [6, 7].

In spite of some investigations [1–7] on the formation, properties and structure of fluorophosphate glasses, data on the crystallization kinetics of these glasses are rare. The determination of the factors affecting the crystallization behaviour of these glasses is necessary if they are to be technologically useful. Otherwise glassy preforms may crystallize during processing or service. An understanding of the crystallization kinetics of these glasses is important also for correlating the crystallization behaviour with glass formation characteristics of the system. Hence, studies on fluorophosphate glasses have both scientific and practical significance.

The kinetic parameters that control the overall nucleation and growth mechanism are shown to depend upon composition in various glass systems [8–12]. Therefore, the kinetic parameters of these glasses are expected to vary with composition. The purpose of this study was to determine the effect of a glass former, $Ba(PO_3)_2$, concentrations and heating rates on the crystallization kinetics of fluorophosphate glasses.

2. Experimental procedures

Six different fluorophosphate glass compositions were prepared for studying the crystallization kinetics. The batch compositions of the glasses are listed in Table I. The raw materials were certified reagent grade and carefully weighed to form a batch of desired glass compositions. The batch materials were dry mixed in a glass jar prior to melting. The weight of each batch ranged from 1 to 10 g depending upon the $Ba(PO_3)_2$ content. For compositions containing $\geqslant 1.5$ mol % $Ba(PO_3)_2$, 10 g of the premixed powders were melted $\sim 900\,^{\circ}C$ for 15 to 20 min in a platinum crucible in an electric furnace. Melting took place under normal laboratory conditions. The molten batch material was quenched by placing the bottom of the crucible in ice water. Due to the high fluidity of the melt, excellent homogeneity was obtained by manually swirling the crucible and contents periodically during melting and just prior to quenching.

For compositions containing < 1.5 mol % $Ba(PO_3)_2$, a strip furnace was used. Glasses were prepared by melting 1 g of the premixed powder in a platinum boat at $\sim 900\,^{\circ}C$ for 2 to 3 min in nitrogen. When melting was complete, the power to the furnace was turned off and helium gas was blown over the platinum boat containing the melt in order to achieve higher cooling rates.

As-quenched samples were analysed by X-ray diffraction (XRD) and by scanning electron microscopy to confirm the glassiness of the samples. Analyses

0022–2461

TABLE I Batch composition of fluorophosphate glasses investigated in this study

Glass no.	Composition (mol %)					
	$Ba(PO_3)_2$	AlF_3	CaF_2	MgF_2	SrF_2	BaF_2
1	5.00	40.00	30.00	10.00	10.00	5.00
2	3.00	40.84	30.64	10.21	10.21	5.10
3	1.50	41.48	31.10	10.37	10.37	5.18
4	0.75	41.78	31.35	10.45	10.45	5.22
5	0.25	42.00	31.50	10.50	10.50	5.25
6	0	42.10	31.58	10.53	10.53	5.26

suggested no evidence of unmelted and crystalline particles in the as-quenched glass.

The quenched glass was ground and screened to 106–150 μm, i.e. particles passed through a sieve of 150 μm openings and remained on that of 106 μm openings. A model 1700, Perkin-Elmer thermoanalyser was used for differential thermal analysis (DTA) and the reference material was Al_2O_3. Heating rates of 2, 4, 6, 10, 15, 20 and 25 °C min^{-1} were used for the DTA measurements. The amount of sample was restricted so that the maximum temperature rise during crystallization did not exceed 2 or 3 °C. The DTA scans were conducted using platinum crucibles in flowing nitrogen at flow rates of 50 cm^3 min^{-1}. The sample weight of $\sim$20 mg is kept constant for all DTA measurements.

The crystallization kinetic parameters were measured using the modified Johnson–Mehl–Avrami (JMA) equation applicable to non-isothermal crystallization [13]. A relation between the temperature at the peak maxima of the crystallization exotherm, T_p, and the heating rate ϕ, has been derived as

$$\ln\frac{T_P^2}{\phi} = \ln\frac{E}{R} - \ln\nu + \frac{E}{RT_P} \quad (1)$$

where E and ν are the effective activation energy and frequency factor for crystallization, respectively, and R is the gas constant. A plot of $\ln(T_P^2/\phi)$ versus $1/T_p$ should yield a straight line [13] whose slope and intercept may be used to calculate E and ν, respectively. The value of the Avrami exponent, n, is determined from the shape of the crystallization exotherm and is related to T_p as [14–16]

$$n = \frac{2.5}{\Delta T} \times \frac{T_P^2}{E/R} \quad (2)$$

where ΔT is the width of the crystallization peak at half maximum. Once the kinetic parameters are known, the overall crystallization process may be understood.

3. Results and discussion

The $Ba(PO_3)_2$ content had a profound effect on the crystallization behaviour of the fluorophosphate glasses. This became apparent early in the investigation when identical experimental conditions, i.e. sample weight, particle size, gas atmosphere, gas flow rate and heating rate, resulted in different T_p for

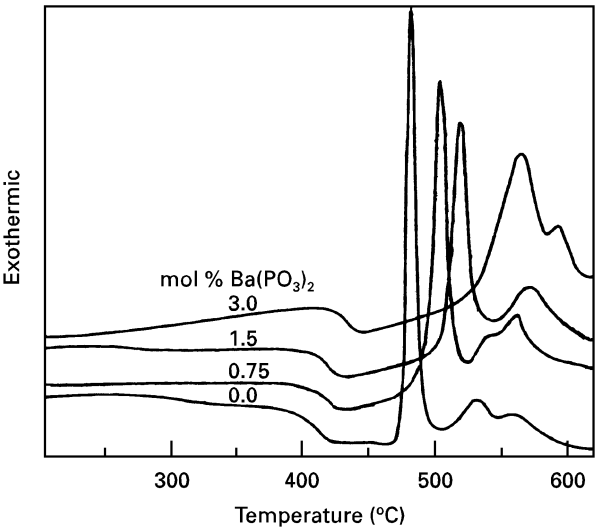

Figure 1 DTA thermograms for fluorophosphate glasses of varying $Ba(PO_3)_2$ content. The heating rate was 10 °C min^{-1}.

samples from different glass compositions. Typical DTA thermograms of the samples containing 0, 0.75, 1.5 and 3 mol % $Ba(PO_3)_2$ are shown in Fig. 1. The crystallization behaviour became more and more complicated with decreasing $Ba(PO_3)_2$ content in the glass. As seen in Fig. 1, the DTA thermograms for the glasses containing 1.5 and 3 mol % $Ba(PO_3)_2$ had two exothermic peaks, and glasses containing < 1.5 mol % $Ba(PO_3)_2$ had three exothermic peaks, one large peak and two smaller peaks at higher temperatures as best seen in the curve for the glass containing no $Ba(PO_3)_2$. The occurrence of the two crystallization peaks on the thermograms was reported also by Macfarlane *et al.* [17] for AlF_3 stabilized ZrF_4 fluoride glasses and was explained as the crystallization of the most unstable phase at lower temperatures. The concomitant concentration changes in the bulk glass drove the remaining glass into a composition region in which it was unstable with respect to other crystalline phases.

It was evident that more than one compound crystallizes from these glasses during heating. The XRD analysis of the samples devitrified during a DTA scan revealed that $CaAlF_5$, $SrAlF_5$, $CaAlF_7$ and $CaSrAlF_7$, crystallize from these glasses when heated. Unfortunately, due to overlapping of the different peaks, it was not possible to identify the crystallizing compound corresponding to each individual exothermic peak.

The DTA thermograms shown in Fig. 1 suggest that the exothermic peak for the glass containing no $Ba(PO_3)_2$ is very sharp, but becomes flatter and shifts to higher temperature as $Ba(PO_3)_2$ content of the glass increased. Also, the height and area of the first exothermic peak decreased with increasing $Ba(PO_3)_2$. A sharp peak is characteristic of the bulk crystallization process; whereas, a broad peak reflects the process of surface crystallization [15]. It is apparent that the crystal growth mechanism changes predominantly from bulk to surface crystallization with increasing $Ba(PO_3)_2$ content.

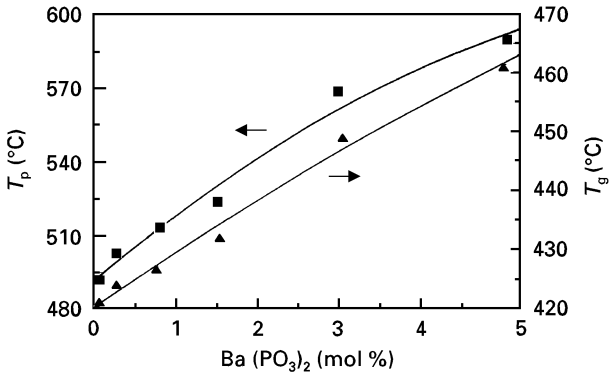

Figure 2 Variation of the temperature at the peak maxima of crystallization exotherm T_P, and glass transition temperature, T_g, with $Ba(PO_3)_2$ concentrations. The heating rate was 10 °C min^{-1}.

The glass transition temperature, T_g, corresponding to the temperature at the minima of the first endotherm, also decreased with increasing $Ba(PO_3)_2$. The variation of T_p and T_g, as a function of $Ba(PO_3)_2$, is shown in Fig. 2. The increase in T_p was ~100 °C while the increase in T_g was ~40 °C for the glass containing 5 mol % $Ba(PO_3)_2$ compared to that containing no $Ba(PO_3)_2$.

The change in the crystallization behaviour of these glasses with a small amount of $Ba(PO_3)_2$ incorporated is due to linking the broken chains present in the structure of fluoride glasses and hence, increasing the ability for glass formation [8]. The structure of fluoride glasses containing AlF_3, CaF_2, MgF_2, SrF_2, and BaF_2 consists of a mixture of linear and branched AlF_6 octahedral chains of various length connected by Ca^{2+}, Mg^{2+}, Sr^{2+} and Ba^{2+} ions [18,19]. Al^{3+} and Mg^{2+} may also form (AlF_4) and (MgF_4) tetrahedras and then reconnect the chains to one another [20]. The improvement in glass formation caused by $Ba(PO_3)_2$ may be explained by the formation of long PO_4 chains in the glass structure. When $Ba(PO_3)_2$ is introduced into the glass, M–F bonds are disrupted and P–F and P–O–P bonds are formed as oxygen replaces fluorine [8]. As a result, the glass network was continuously modified by PO_4 chains.

The IR spectrum of the glass samples and the corresponding devitrified samples were measured to determine the basic structural groups. A portion of the IR spectra of selected fluorophosphate glasses and their crystallization products suggested that the structure changed gradually from short AlF_6 groups to long PO_3F and Ba(Ca, Mg, Sr)P_2O_7, the complex phosphate groups, as seen in Fig. 3. The IR spectra of the glasses resembled those of the corresponding devitrified products although the absorption peaks for the glasses were not as sharp as those of crystallized products. This implies that the basic structural groups remain unchanged during crystallization [8]. A comparison of the spectra for the crystallization products from glasses containing 5 mol % $Ba(PO_3)_2$ and no $Ba(PO_3)_2$ revealed that the IR spectrum of the crystallization products changed, i.e. the number of bands in the spectrum increased, with increasing $Ba(PO_3)_2$. This might be due to the formation of the pyrophosphate structural groups, and gradual symmetrization

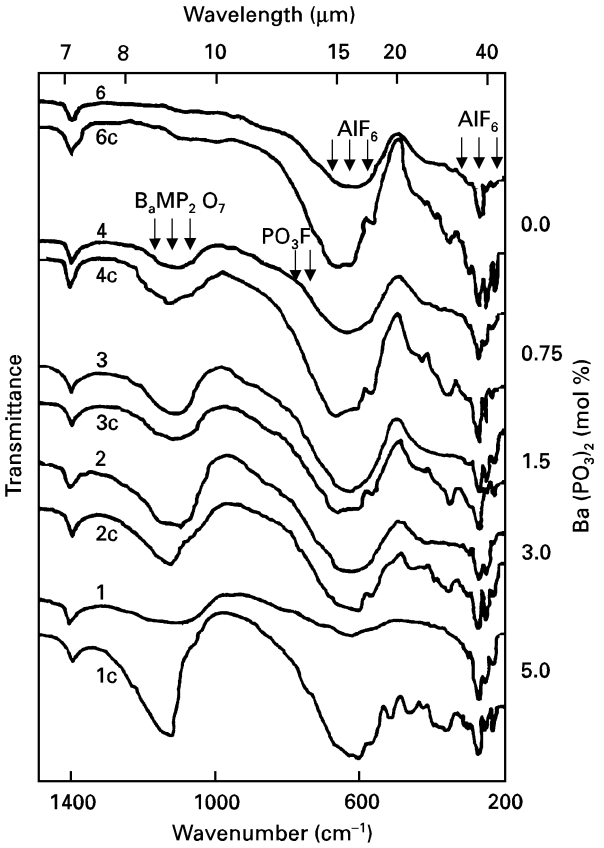

Figure 3 IR transmission spectra of fluorophosphate glasses (6, 4, 3, 2, 1) investigated in this study and their crystallization products (6c, 4c, 3c, 2c, 1c). Compositions in mol % are given in Table I. Curves are arbitrarily displaced along the vertical axis for clarity.

of the structural units of the phosphates [8]. The linking of PO_4 groupings within the AlF_6 octohedral chains impeded the crystallization process.

Heating rates affected the crystallization behaviour of fluorophosphate glasses. T_p shifted to higher temperatures with increasing heating rate. Similar behaviour has been observed for lithia–silica glasses [9] where it is reported that a high heating rate can induce a high crystal growth rate resulting in a high glass–crystal interface temperature which shifts T_p to a temperature higher than that expected from the data for lower heating rates. The variation of crystallization behaviour as a function of heating rate for glass containing 3 mol % $Ba(PO_3)_2$ is shown in Fig. 4. From the appearance of two peaks for the heating rates 4 and 10 °C min^{-1} and a single peak for 20 °C min^{-1}, it was evident that the heating rate 20 °C min^{-1} was faster than the rate of crystallization process for this glass. An increase in T_p and T_g with increasing heating rate was also apparent in Fig. 4. The increase in T_p and T_g with heating rate are separately shown for the glass containing 1.5 mol % $Ba(PO_3)_2$ in Fig. 5.

The effect of the heating rate on the crystallization behaviour of these glasses may be explained by the formation of additional internal nuclei during the DTA scan. At a particular heating rate, the T_p for a glass depends upon the total concentration of surface and internal (bulk) nuclei present in the glass and decreases with increasing concentration of nuclei [11]. If a glass is not initially saturated with internal nuclei,

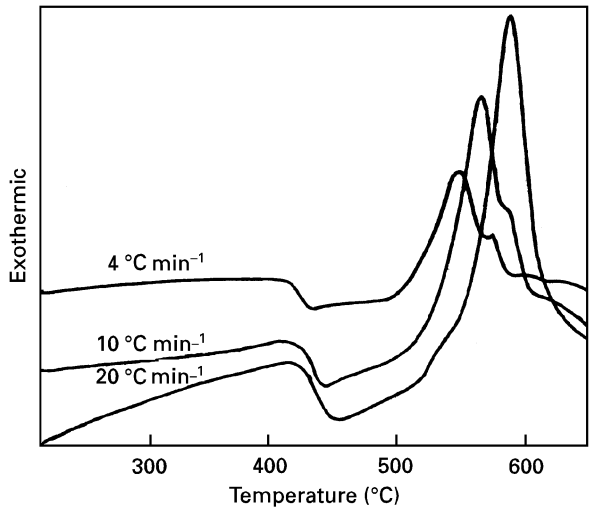

Figure 4 DTA thermograms for fluorophosphate glass containing 3 mol % $Ba(PO_3)_2$ for different heating rates.

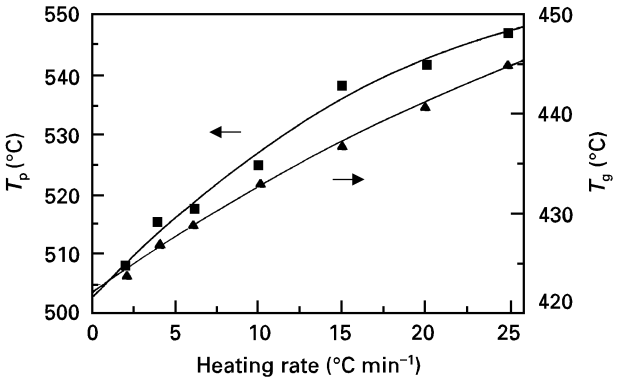

Figure 5 Variation of the temperature at the peak maxima of crystallization exotherm, T_P, and glass transition temperature, T_g, with heating rates for fluorophosphate glass containing 1.5 mol % $Ba(PO_3)_2$.

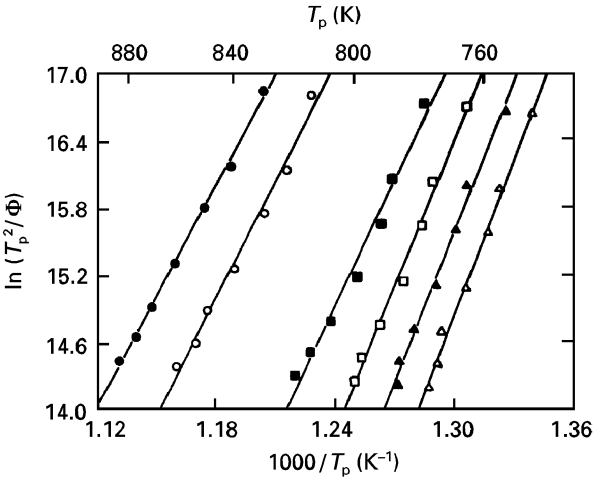

Figure 6 Typical $\ln(T_P^2/\phi)$ versus $1/T_p$ plots for fluorophosphate glasses of varying $Ba(PO_3)_2$ content. Key: ● 5 mol % $Ba(PO_3)_2$; ○ 3 mol % $Ba(PO_3)_2$; ■ 1.5 mol % $Ba(PO_3)_2$; □ 0.75 mol % $Ba(PO_3)_2$; ▲ 0.25 mol % $Ba(PO_3)_2$; △ 0 mol % $Ba(PO_3)_2$.

TABLE II Values of kinetic parameters for fluorophosphate glasses investigated in this study

$Ba(PO_3)_2$ (mol %)	$E \pm 10$ (kJ mol^{-1})	ν (s^{-1})	$n \pm 0.5$
0.00	377	6.98×10^{23}	3.9
0.25	365	5.02×10^{22}	3.8
0.75	352	2.80×10^{21}	3.6
1.50	303	4.90×10^{17}	3.4
3.00	284	3.39×10^{15}	1.6
5.00	268	1.28×10^{14}	1.5

additional internal nuclei can form during a DTA scan, the concentration of which will be higher for slower heating rates, since the glass spends a longer time in the temperature range where nucleation can occur [11]. The concentration of the nuclei decreases with increasing heating rate since less time is spent in the nucleation range. The difference in the nuclei concentration between low and high heating rates increases. Therefore, T_p for higher heating rates shifts to higher temperatures. Evidently, bulk nucleation was dominant at low heating rates and each particle grew three-dimensionally. The contribution of surface crystallization increased as the heating rate increased.

The $\ln(T_P^2/\phi)$ versus $1/T_p$ plots for fluorophosphate glasses investigated are shown in Fig. 6. The solid lines are the least squares fit of the data points. The experimental data points are in a good agreement with the theory. The kinetic parameters, E and ν, of these glasses were determined from the slope and intercept, respectively, of the straight lines and are listed in Table II. Values of n were computed from Equation 2 and are also listed in Table II. The variation of the kinetic parameters as a function of $Ba(PO_3)_2$ are shown in Fig. 7. E, ν and n decreased with increasing $Ba(PO_3)_2$ content, or in other words, with increasing glass former (P_2O_5) concentrations. E, ν and n decreased from 377 ± 10 kJ mol^{-1}, 6.98×10^{23} s^{-1} and 3.9 ± 0.5, respectively, to 268 ± 10 kJ mol^{-1}, 1.28×10^{14} s^{-1} and 1.5 ± 0.5 as $Ba(PO_3)_2$ increased from 0 to 5 mol %. Lower values of E for the modified glasses compared to the parent glass indicate that the modified glasses are more stable and have higher resistance to devitrification [21]. The decrease in E with increasing $Ba(PO_3)_2$ is interpreted as an indication of increasing tendency for glass formation of the modified glass [12]. Although it is difficult to find the physical meaning of the activation energy precisely when bulk and surface crystallization occur simultaneously [22] a decrease in E indicates a changing crystallization process from bulk to surface which has also been reflected in the shape of the crystallization exotherms as discussed earlier. Bansal *et al.* [14] reported that a value of n close to three suggests a constant number of nuclei growing spherically in three dimensions at a constant rate. The decrease in n from 3.9 to 1.5 as $Ba(PO_3)_2$ increases from 0 to 5 mol % is also evidence of the change in crystallization behaviour from bulk to surface. No crystallization data is available in the literature for these glasses with which the results from the present investigation can be directly compared. However, a bulk nucleation and three-dimensional growth was reported for Ba–La–Zr–Al fluoride glasses [17].

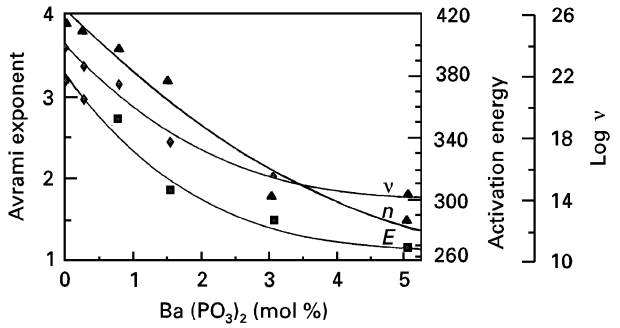

Figure 7 Variation in Avrami exponent, *n*, activation energy, *E*, and frequency factor, ν, for crystallization as a function of $Ba(PO_3)_2$ for fluorophosphate glasses.

4. Conclusions

1. Bulk crystallization and surface crystallization occurred simultaneously in fluorophosphate glasses. Incorporation of a small amount of $Ba(PO_3)_2$ changed the crystallization behaviour of these glasses from bulk to surface.

2. Bulk nucleation was dominant at low heating rates. The contribution of surface crystallization increased with increasing heating rate.

3. The IR transmission analysis of selected fluorophosphate glasses and their crystallization products revealed that the structure changed gradually from short chains of AlF_6 groups to the long chains of PO_3F and Ba(Ca, Mg, Sr)P_2O_7 groups with increasing $Ba(PO_3)_2$ content.

4. The XRD analysis revealed that $CaAlF_5$, $SrAlF_5$, $CaAlF_7$ and $CaSrAlF_7$ crystallize from these glasses when heated.

References

1. J. T. WENZEL, D. H. BLACKBURN, W. K. HALLER, S. STOWSKI and M. J. WEBER, *Soc. Photo-Opt. Instrum. Eng.* **204** (1979) 59.
2. B. KUMAR and R. HARRIS, *Phys. Chem. Glasses* **25** (1984) 155.
3. P. A. TICK, *J. Amer. Ceram. Soc.* **66** (1983) 716.
4. J. YASI, J. FUSONG and G. FUXI, *Chin. Phys.* **3** (1983) 162.
5. M. SAMMET and R. BRUCKNER, *Glastech. Ber.* **58** (1985) 106.
6. R. K. SANDWICK, R. J. SCHELLER and K. H. MADER, *Soc. Photo-Opt. Instrum. Eng.* **171** (1979) 161.
7. B. KUMAR, *Mater. Res. Bull.* **16** (1981) 179.
8. A. OZTURK, Ms thesis, University of Missouri-Rolla, USA (1987).
9. C. S. RAY, W. HUANG and D. E. DAY, *J. Amer. Ceram. Soc.* **70** (1987) 599.
10. N. P. BANSAL, A. J. BRUCE, R. H. DOREMUS and C. T. MOYNIHAN, *J. Non-Cryst. Solids* **70** (1985) 379.
11. C. S. RAY and D. E. DAY, *J. Amer. Ceram. Soc.* **67** (1984) 806.
12. *Idem*, *J. Non-Cryst. Solids* **81** (1986) 173.
13. N. P. BANSAL, *J. Therm. Anal.* **29** (1984) 115.
14. N. P. BANSAL, R. H. DOREMUS, A. J. BRUCE and C. T. MOYNIHAN, *J. Amer. Ceram. Soc.* **66** (1983) 233.
15. C. S. RAY, W. HUANG and D. E. DAY, *ibid.* **74** (1991) 60.
16. J. A. AUGIS and J. D. BENETT, *J. Therm. Anal.* **13** (1978) 283.
17. D. R. MACFARLANE, M. MATECKI and M. POULAIN, *J. Non-Cryst. Solids* **64** (1984) 351.
18. D. EHRT and W. WOGEL, *Z. Chem.* **23** (1982) 111.
19. D. EHRT, H. ERDMANN and W. WOGEL, *ibid.* **23** (1983) 37.
20. G. FUXI, J. YASI and J. FUSONG, *J. Non-Cryst. Solids* **52** (1982) 263.
21. N. P. BANSAL, A. J. BRUCE, R. H. DOREMUS and C. T. MOYNIHAN, *ibid.* **70** (1985) 379.
22. MATUSITA and S. SAKKA, *Bull. Inst. Chem. Res.* **59** (1981) 159.

Received 19 April
and accepted 19 November 1996